The Impacts of Radio Channels and Node Mobility on Link Statistics in Mobile Ad Hoc Networks

Ming Zhao Wenye Wang

Department of Electrical and Computer Engineering
North Carolina State University
Raleigh, North Carolina 27695–7911
Email: {mzhao2, wwang}@ncsu.edu

***Abstract*— Understanding link statistics in mobile ad hoc networks (MANETs) is essential to design adaptive routing protocols and achieve desired network performance. While much attention has been given to the node mobility impacts, little has been done to investigate the influence of dynamic channel fadings and the joint effects of the interactions among radio channels, transmission range, node mobility and node-pair distance on link statistics. In this paper, we investigate the *link stability* and *availability* by using a distance transition probability matrix of a relative distance between two nodes. Our analysis takes the node effective transmission range R_e into account. The relative node movement is based on the Semi-Markov Smooth (SMS) mobility model [1] which captures the smooth node speed (V) transition and the radio channel variations in a small time-scale. We show that the PDF of link lifetime in MANETs can be effectively approximated by the exponential distribution characterized by the parameter V/R_e. Moreover, we find that the impacting factors on residual link lifetime are in the decreasing order of node speed, transmission range, node-pair distance. The analytical results are validated by extensive simulations.**

I. Introduction

The dynamic node mobility and harsh wireless environment lead to frequent link failures in mobile ad hoc networks (MANETs). As the routing performance highly depends on their adaptability to the link dynamics, adaptive routing with respect to frequent link and topology changes is an essential prerequisite to achieve desired network performance and fulfill the potential QoS required services in MANETs. Therefore, the study of link statistics can effectively reveal necessary information of the underlying routing and network performance.

A wide body of studies on link statistics which are used to measure the stability [2]–[5] and availability [2], [6], [7] of links in MANETs has been proceeded recently. All these studies of link statistics are based on random mobility models [8]. While random mobility models assume that the speed and direction keep constant within each movement, they are not sufficient to capture smooth speed and direction change of mobile nodes during one movement. Because of this constraint, the relative velocity between two nodes may not vary during the entire link connection [4], which is contrary to the reality, as nodes may change their speed and direction as frequently as possible during their moving. Furthermore, the node velocity in random mobility models has no correlation between two consecutive time epochs. Thus, these models frequently generate abrupt moving behaviors such as sudden stop and sharp turn which are not in comply with smooth motions in real world [1]. In consequence, the characteristics of the relative velocity between a node pair based on random mobility models may be biased, which could further lead to inaccurate theoretical and simulation results on link statistics.

Though much attention has been focused on the node mobility effects on link statistics, little has been done to investigate how dynamic wireless environments influence the link performance. Without considering the factor of channel fadings, the transmission range is taken a fixed value for granted in most existing studies. Thus, the link status is deterministic regarding a fixed node-pair distance. While, in reality, a received signal of a mobile node is generally influenced by three fading effects: large-scale path loss, multipath, and shadowing [9]. The link status may vary greatly in different time-varying wireless environments, even the node-pair distance is same.

By observing these two limitations, we are motivated to investigate the link statistics upon (i) a *microscopic mobility model* which can capture the temporal correlation of smooth velocity transition in a small time-scale [10] and (ii) a *dynamic* transmission range regarding the characteristics of mobile wireless environments [11]. Meanwhile, the link properties strongly depend on the relative movement, which in turn depends on the node-pair distance. Therefore, in this paper, we aim to conduct an in-depth study of the stochastic link properties according to the interactions among channel fadings, transmission range, node mobility, and node-pair distance. Specifically, we study the link statistics in terms of the *link stability* characterized by expected link lifetime and the *link availability* indicated by link residual lifetime. We utilize a distance transition probability matrix for modeling the relative distance variation after every discrete time step. Our analytical scheme, results and findings on link statistics can be readily served as bases for on-going research in MANETs.

The remainder of the paper is organized as follows. Section II analyzes the effective transmission range upon radio channel fadings. Section III characterizes the relative movement of two nodes under the SMS mobility model and describes all preliminaries necessary for analyzing link statistics. In Section IV, we elaborate the analysis of link stability and availability. Section V concludes this paper.

1930-529X/07/$25.00 © 2007 IEEE
This full text paper was peer reviewed at the direction of IEEE Communications Society subject matter experts for publication in the IEEE GLOBECOM 2007 proceedings.

II. Effective Transmission Range

In MANETs, different links may experience very different channel fading. In general, the received signal of a mobile node is influenced by three fading effects: large-scale path loss, multipath and shadowing. Let P_r and P_t be the receiving and the transmitting signal power, respectively. By considering these three fading effects, the pass loss PL of the signal during the transmission is represented in decibel (dB) as [9]:

$$\begin{cases} PL_{dB} = \overline{L}_{0,dB} + 10\xi \log_{10}(d) + X_{\sigma_s} + 10\log_{10}\chi^2 \\ P_{r,dB} = P_{t,dB} - PL_{dB}, \end{cases} \quad (1)$$

where ξ is the path loss exponent, $\overline{L}_{0,dB}$ is the average path loss at the reference point that is 1 meter away from the transmitter. d denotes the node pair distance. X_{σ_s} is the shadow fading random variable, measured in dB, which is a zero-mean Gaussian variable with variance σ_s^2. χ^2 models the multipath fading. In detail, $f_\chi(\chi)$ has a Rayleigh density, adjusted by the parameter ${\sigma_r}^2$, so that $E\{\chi^2\} = 2{\sigma_r}^2$ [9].

Fig. 1 illustrates an example of the probability of link connection between two nodes under different fading conditions. Regarding the large-scale path loss only, we assume that two nodes are always connected if their distance is less than 200 m. At this distance threshold, it is observed that the probability of link connection decreases from 1 to 0.5 when the additional shadow fading is considered, and it further reduces to 0.28 if all these three propagation mechanisms are in effect. Clearly, the node transmission range, i.e., the maximum node-pair distance which guarantees the effective signal communication, becomes a random variable features by the radio channel characteristics.

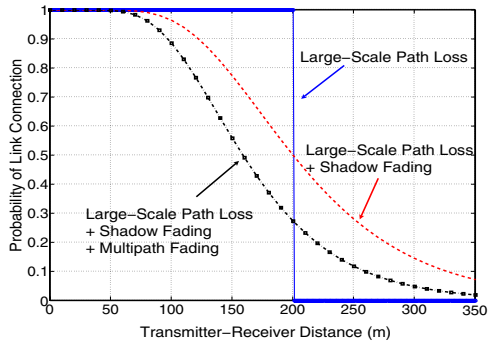

Fig. 1. Probability of link connection between two nodes, where path loss exponent is $\xi = 3$, shadow fading $\sigma_s = 5$ dB, and multipath fading is 3 dB.

It is showed that the link and connectivity analysis given the geometric disc abstraction generally holds for more irregular shapes of a node transmission zone [12]. Thus, we introduce *Effective Transmission Range* (ETR) to capture the effect of radio propagation mechanisms on received signal strength.

Definition 1: In a radio channel characterized by the path loss exponent ξ, shadowing X_{σ_s} and multipath fading χ^2, given the threshold of receiving power $P_{0,dB}$, the *Effective Transmission Range* ($ETR = R_e$) is the maximum value of R, which holds the condition $P_{r,dB} \geq P_{0,dB}$ with a very high probability ("almost surely" [11]) $\mathbb{P} = 99\%$.

Let $\tilde{P}_{dB} = P_{t,dB} - \overline{L}_{0,dB} - 10\log_{10}\chi^2$, from (1), we have

$$\begin{aligned} \mathbb{P} &= Pr\{\tilde{P}_{dB} - 10\xi\log_{10}R_e - X_{\sigma_s} \geq P_{0,dB}\} \\ &= \frac{1}{\sqrt{2\pi}\sigma_s}\int_{-\infty}^{\tilde{P}_{dB}-10\xi\log_{10}R_e - P_{0,dB}} exp(-\frac{x^2}{2{\sigma_s}^2})dx \\ &= \frac{1}{2}[1 - erf(\frac{10\xi\log_{10}R_e + P_{0,dB} - \tilde{P}_{dB}}{\sqrt{2}\sigma_s})], \end{aligned} \quad (2)$$

where $erf(\cdot)$ is the error function, defined by $erf(z) = \int_0^z \frac{2}{\sqrt{\pi}}e^{x^2}dx$. From the Definition 1, we have

$$\begin{cases} \frac{1}{2}[1 - erf(\frac{10\xi\log_{10}R_e + P_{0,dB} - \tilde{P}_{dB}}{\sqrt{2}\sigma_s})] = 0.99, \\ \frac{10\xi\log_{10}R_e + P_{0,dB} - \tilde{P}_{dB}}{\sqrt{2}\sigma_s} = -1.65. \end{cases} \quad (3)$$

Hence, upon (3), we obtain the ETR R_e of mobile nodes with specific requirements in a wireless environment as:

$$\log_{10}R_e = \frac{-2.33\sigma_s + \tilde{P}_{dB} - P_{0,dB}}{10\xi}. \quad (4)$$

If we assume that each node uses same transmission power and receiving power threshold, then $P_{t,dB} - \overline{L}_{0,dB} - P_{0,dB}$ is a constant value denoted by c. From (4), it is evident that R_e is a function of three fading parameters:

$$R_e = f(\xi, \sigma_s, \chi) = 10^{\frac{-2.33\sigma_s - 10\log_{10}\chi^2 + c}{10\xi}}. \quad (5)$$

Based on the derivation of ETR R_e from (4) and (5), next we will describe all preliminaries necessary for analyzing link stochastic properties.

III. Relative Movement and Preliminaries

Besides the impacts of wireless channel fadings on link dynamics, a valid mobility model for MANET link study should describe the smooth temporal correlation of node velocities [1], but also capture the minute variation of node velocity in small time-scale, in order to match the time-scale variation of radio channels [10]. Therefore, in this paper, we select the *Semi-Markov Smooth* (SMS) mobility model proposed in [1] for analyzing link properties. In detail, for each SMS movement, a node will randomly select a target direction ϕ_α and a target speed v_α as the expected direction and speed of the movement. Each SMS movement contains a random number of equal-length *time steps* (Δt)s. Specifically, an SMS movement contains three consecutive moving phases: Speed Up phase for even speed acceleration from 0 m/s to v_α; Middle Smooth phase for maintaining stable velocities which respectively fluctuate around v_α and ϕ_α in each time step; and Slow Down phase for even speed deceleration to 0 m/s. Next, we investigate the characteristics of the relative movement based on the SMS model.

A. Relative Movement and Distance Pattern

Fig. 2 illustrates an example relative movement trajectory between a node-pair (u, w). As the reference node, node u lies in the center of its own transmission zone with radius characterized by $ETR = R_e$. We denote v_m as the magnitude

1930-529X/07/$25.00 © 2007 IEEE
This full text paper was peer reviewed at the direction of IEEE Communications Society subject matter experts for publication in the IEEE GLOBECOM 2007 proceedings.

of the relative speed vector $\overrightarrow{v}_m$. After the m^{th} time step relative movement, node w lies at the position represented by (X_m, Y_m). Correspondingly, ρ_m is the magnitude of the vector $\overrightarrow{\rho}_m$, representing the node-pair distance, such that $\rho_m = \sqrt{{X_m}^2 + {Y_m}^2}$. Here, the relative speed v_m and the angle ψ_m of node w are i.i.d. RVs.

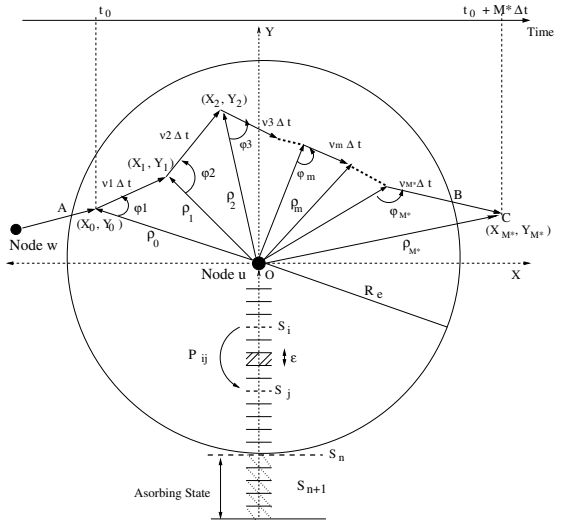

Fig. 2. Relative movement trajectory of node pair (u, w).

B. Distance Transition Probability Matrix $\mathbf{P}$

We denote $\mathbf{P}$ as the distance transition probability matrix, to model the distance transition at each time step. In detail, let the R_e of node u be quantized into n equal-length intervals with a width of ε meters. Hence, $R_e = n \cdot \varepsilon$, that means there are n states within node u's transmission zone. Each element P_{ij} indicates the transition probability that u-w distance is changed from state S_i to state S_j after one time step. From Fig. 2, the link expires after the M^{*th} time step when the event of $\{\rho_{M^*} > R_e\}$ first happens. In addition, we use state S_{n+1} to represent all the u-w distances that are over R_e. Since link connection breaks when node w reaches state S_{n+1}, we define state S_{n+1} as the *absorbing state* of matrix $\mathbf{P}$. This implies that $\mathbf{P}$ is an n by $n+1$ matrix.

C. Single-step Transition Probability P_{ij} Approximation

The transition probability of P_{ij} of matrix $\mathbf{P}$ is essential to the analytical study of link statistics because it directly indicates the potential variation of node-pair distance within one time step according to the relative node speed. In our previous study [13], P_{ij} is derived as follows:

$$\begin{cases} P_{ij} = \frac{\int_{(j-1)\varepsilon}^{j\varepsilon} \int_{(i-1)\varepsilon}^{i\varepsilon} f_{\rho_m|\rho_{m-1}}(\rho_m|\rho_{m-1}) f(\rho_{m-1}) d\rho_{m-1} d\rho_m}{\int_{(i-1)\varepsilon}^{i\varepsilon} f(\rho_{m-1}) d\rho_{m-1}} \\ f(\rho_m|\rho_{m-1}) = \int_0^{2(v_\alpha+\delta_v)} \frac{\frac{\rho_m}{{v_\alpha}^2} \cdot v \cdot e^{(\frac{-\pi v^2}{4{v_\alpha}^2})} dv}{\left[4\rho_{m-1}^2\rho_m^2 - \left[v^2 - (\rho_{m-1}^2+\rho_m^2)\right]^2\right]^{1/2}}, \end{cases} \quad (6)$$

where v_α represents the target stable speed of a node movement and δ_v is the maximum speed variation of v_α in one time step [13]. Although (6) has no closed-form for the expression of P_{ij}, we find that a highly accurate approximation of P_{ij} can be achieved [1]. In detail, based on the *Schwarz Inequality*, i.e., $\int_a^b |f(x) \cdot g(x)| dx \le \left[\int_a^b |f(x)|^2 dx\right]^{\frac{1}{2}} \left[\int_a^b |g(x)|^2 dx\right]^{\frac{1}{2}}$, $f_{\rho_m|\rho_{m-1}}(\rho_m|\rho_{m-1})$ in (6) has the inequality:

$$\begin{aligned} f_{\rho_m|\rho_{m-1}}(\rho_m|\rho_{m-1}) &\le \frac{\rho_m}{2{v_\alpha}^2} \left[\int_0^{4(v_\alpha+\delta_v)^2} e^{(\frac{-\pi x}{2{v_\alpha}^2})} dx\right]^{\frac{1}{2}} \\ &\quad \times \left[\int_0^{4(v_\alpha+\delta_v)^2} \frac{dx}{4\rho_{m-1}^2\rho_m^2 - \left[x - (\rho_{m-1}^2+\rho_m^2)\right]^2}\right]^{\frac{1}{2}} \\ &\le \frac{0.2}{v_\alpha}\sqrt{\frac{\rho_m}{\rho_{m-1}}} \left[\ln \frac{|4(v_\alpha+\delta_v)^2 - (\rho_m-\rho_{m-1})^2|(\rho_{m-1}+\rho_m)^2}{|(\rho_{m-1}+\rho_m)^2 - 4(v_\alpha+\delta_v)^2|(\rho_m-\rho_{m-1})^2}\right]^{\frac{1}{2}}. \quad (7) \end{aligned}$$

We further apply the Mean-Value theorem in Calculus to derive the numerical solution of P_{ij}. Assume that the number of states n of the matrix $\mathbf{P}$ is larger enough, i.e., ε is sufficiently small, we can effectively use the middle point $i - \frac{\varepsilon}{2}$ and $j - \frac{\varepsilon}{2}$ to respectively represent the value of ρ_{m-1} and ρ_m. For instance, $\int_{(i-1)\varepsilon}^{i\varepsilon} f(\rho_{m-1}) d\rho_{m-1} \approx \varepsilon \cdot f(i\varepsilon - \frac{\varepsilon}{2})$. Upon this argument and the result from (7), P_{ij} derived in (6) can be effectively approximated by $\tilde{P}_{ij}$ as follows:

$$\begin{aligned} \tilde{P}_{ij} &\approx \varepsilon \cdot f_{\rho_m|\rho_{m-1}}[(j - \frac{1}{2}) \cdot \varepsilon \mid (i - \frac{1}{2}) \cdot \varepsilon)] \\ &\approx \frac{0.2\varepsilon}{v_\alpha}\sqrt{\frac{2j-1}{2i-1}} \left[\ln \frac{|4(v_\alpha+\delta_v)^2 - \varepsilon^2(j-i)^2|(i+j-1)^2}{|\varepsilon^2(i+j-1)^2 - 4(v_\alpha+\delta_v)^2|(j-i)^2}\right]^{\frac{1}{2}}. \end{aligned} \quad (8)$$

Furthermore, to guarantee the fundamental property of the transition matrix $\mathbf{P}$, i.e., $\sum_j P_{ij} = 1$, the approximation value of $\tilde{P}_{ij}$ is normalized along each row of the matrix $\mathbf{P}$.

IV. Link Statistics

In this section, we analyze link statistics in terms of link stability and availability by joint consideration of the effective transmission range and relative node movement.

A. Link Stability and Link Lifetime

Link stability indicates how stable a link is and how long the link lasts in a mobile wireless environment. Hence, Link stability can be manifested by the expected link lifetime, which is characterized by the distribution of link lifetime.

Let T_L denote the link lifetime, which is the time node w continuously lies inside node u's transmission zone. Upon Fig. 2, the link expires after the M^{*th} time step. In this example, $T_L = M^*\Delta t$, hence T_L is a random variable and the CDF of link lifetime is $Prob\{T_L \le m\}$ for $\Delta t = 1$ s. We denote $\pi_i^{(m)}$ as the probability that node w lies in state S_i after the m^{th} step, and $\pi^{(m)}$ be the row vector whose i^{th} element is $\pi_i^{(m)}$. That is $\pi^{(m)} = \left(\pi_1^{(m)}, \cdots, \pi_i^{(m)}, \cdots, \pi_{n+1}^{(m)}\right)$. And $\pi^{(0)}$ denotes the probability of the initial state that node w lies when the link is initially formed. Upon Fig. 2, $\pi_i^{(0)} = Prob\{\rho_0 \in S_i\}$. For simplicity, we denote matrix $\mathbf{P}$ as $\mathbf{P} = [P_1, \cdots, P_j, \cdots, P_{n+1}]$ and P_j is the j^{th} column vector of $\mathbf{P}$. That means, $P_j = [P_{1j}, P_{2j}, \cdots, P_{ij}, \cdots, P_{(n+1)j}]^T$. where P_{ij} is approximated from (8).

[1] According to our simulation results, ε takes the value of 1 m for $v_\alpha \ge 10$ m/s; otherwise, $\varepsilon = v_\alpha/10$ m can satisfy the high accuracy requirement.

1930-529X/07/$25.00 © 2007 IEEE

Because S_{n+1} is the absorbing state of the matrix $\mathbf{P}$, $[\pi^{(0)}\mathbf{P}^m]_{(n+1)}$ represents the probability that node w moves outside node u's transmission zone R_e within m time steps. Then, with the knowledge of $\pi^{(0)}$ and $\mathbf{P}$, the CDF of link lifetime can be obtained by:

$$Prob\{T_L \leq m\} = [\pi^{(0)}\mathbf{P}^m]_{(n+1)} = \pi^{(m)}_{n+1}. \quad (9)$$

From (9), the PMF of link lifetime distribution is given by:

$$\begin{aligned} Prob\{T_L = m\} &= Prob\{T_L \leq m\} - Prob\{T_L \leq m-1\} \\ &= [\pi^{(0)}\mathbf{P}^m]_{(n+1)} - [\pi^{(0)}\mathbf{P}^{m-1}]_{(n+1)}. \end{aligned} \quad (10)$$

With (10), the expected link lifetime, i.e., the link stability denoted by $\overline{T}_L$, is represented as:

$$\overline{T}_L = \sum_{m=1}^{\infty} m([\pi^{(0)}\mathbf{P}^m]_{(n+1)} - [\pi^{(0)}\mathbf{P}^{m-1}]_{(n+1)}). \quad (11)$$

In order to validate the analytical results of (10) and (11), we carried out multiple trials with 50 nodes in SMS model with $R_e = 250$ m distributed in an area of 1401m $\times$1401m during a time period of 1000 seconds. Node mobility is set to zero pause time, 0.5 for the temporal correlation parameter, $[20, 40]$ seconds for the middle smooth phase duration, and $[4, 6]$ seconds for speed up and slow down phase durations.

Fig. 3(a) illustrates the link lifetime distribution with two mobility levels: low level ($v_\alpha = 2$ m/s) and high level ($v_\alpha = 20$ m/s). For clear demonstration, we show the results in the log-scale on Y-axis. Both theoretical and simulation results demonstrate that link lifetime *decreases exponentially* with time regardless of the node speed and it decreases much quickly as the node speed is high.

As shown in Fig. 3(b), the theoretical results of $\overline{T}_L$ from (11) fit very well with the simulation results. More interestingly, we find that the $\overline{T}_L$ can be effectively estimated by the empirical equation $\hat{T}_L = R_e/v_\alpha$. Table I illustrates the results of both theoretical $\overline{T}_L$ from (11) and estimated $\hat{T}_L$ with respect to node mobility, where $R_e = 250$ m.

TABLE I
COMPARISON: THEORETICAL $\overline{T}_L$ AND ESTIMATED $\hat{T}_L$

$v_\alpha(m/s)$	2	5	10	15	20	25
$\overline{T}_L(s)$	118.20	53.75	26.35	21.23	16.92	14.28
$\hat{T}_L(s)$	125	50	25	16.67	12.5	10

We already observed that the PMF of link lifetime decreases exponentially with time in Fig. 3(a) and the link stability $\overline{T}_{link} \approx R_e/v_\alpha$ in Table I, respectively. Therefore, the PDF of link lifetime with continuous time t can be approximated by an exponential distribution with parameter $\frac{v_\alpha}{R_e}$, that is

$$\begin{aligned} f_{T_L}(t) &\approx \frac{v_\alpha}{R_e} \cdot e^{(-\frac{v_\alpha \cdot t}{R_e})}, \\ &= \frac{v_\alpha}{f(\xi, \sigma_s, \chi)} \cdot e^{(-\frac{v_\alpha \cdot t}{f(\xi, \sigma_s, \chi)})}. \end{aligned} \quad (12)$$

It can be seen in Fig. 3(c) that this approximated exponential distribution characterized by the parameter $\frac{v_\alpha}{R_e}$, matches very well with the simulation results, especially for high speed. Recall, $R_e = f(\xi, \sigma_s, \chi)$, defined in (5), is a function of

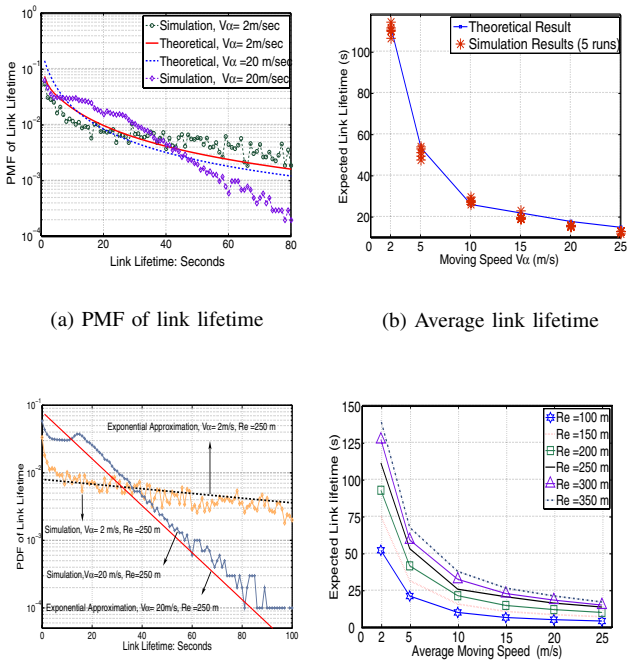

(a) PMF of link lifetime (b) Average link lifetime

(c) PDF Approximation (d) ETR impacts

Fig. 3. Stocastic properties of link lifetime.

radio channel parameters: path loss (ξ), shadow fading (X_{σ_s}), and multi-path fading (χ^2). Hence, the parameter $\frac{v_\alpha}{R_e}$ in (12) indicates that the link performance in mobile wireless network is characterized by joint effects of radio channels and node mobility. Therefore, the value of $\frac{v_\alpha}{R_e}$ can be regarded as a crucial metric for evaluating link performance in MANETs.

Furthermore, upon the analytical result in (11), we investigate the ETR effect on the link stability $\overline{T}_L$ according to different node mobility, the results are shown in Fig. 3(d). We find that the larger R_e is, the longer $\overline{T}_L$ is obtained, which is consistent with our intuition. However, the ETR has much more significant impact on link stability for nodes with low mobility than those with high mobility. This result implies that for an ad hoc network with lower node mobility, or even without node mobility such as a static sensor network, the ETR, i.e., the radio channel features, predominates the link stability $\overline{T}_L$. While for a network with faster mobile nodes such as vehicular ad hoc network (VANET), the link stability $\overline{T}_L$ is dominated by the node mobility.

B. Link Availability and Residual Link Lifetime

Compared to the metric of link stability, *link availability* is a general term to measure the capability that the link resource between a node pair is continuously available given the current link existence. Thus, link availability is manifested by the distribution of residual link lifetime. Different from previous studies [6], [7], we utilize the information of relative distance associated with transition matrix $\mathbf{P}$ to increase the prediction of link availability. Specifically, we define *link availability* $L(\rho_m^{(i)}, m')$, as the probability that the u-w link is continuously available m' steps given the link is available at m^{th} time step

when the relative distance ρ_m is in state S_i. Hence, the link availability is defined as

$$L(\rho_m^{(i)}, m') = \frac{Prob\{T_L \geq m' + m\}}{Prob\{T_L > m \mid \rho_m \in S_i\}}. \quad (13)$$

Here, the given condition $\rho_m \in S_i$ indicates that after the m^{th} step, the probability $Prob\{\rho_m \in S_i\} = 1$. Correspondingly, let $\pi_{i,1}^{(m)}$ be the distribution vector in which the i-th element is equal to 1, while other elements are equal to 0. With the knowledge of link availability $L(\rho_m^{(i)}, m')$, the PMF of residual link lifetime T_R, which is defined as the probability that $\{\rho_{m+m'} \leq R_e \cap \rho_{m+m'+1} > R_e\}$ given that $\{\rho_m \leq R_e\}$ at the m^{th} time step, can be presented as

$$\begin{aligned} Prob\{T_R = m'\} &= L(\rho_m^{(i)}, m' - 1) - L(\rho_m^{(i)}, m') \\ &= [\pi_{i,1}^{(m)} \mathbf{P}^{m'}]_{(n+1)} - [\pi_{i,1}^{(m)} \mathbf{P}^{m'-1}]_{(n+1)}. \end{aligned} \quad (14)$$

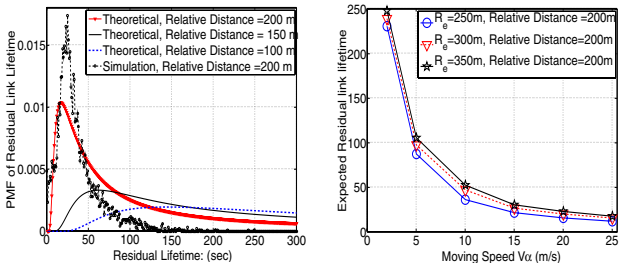

(a) Initial node-pair distance (b) ETR impacts

Fig. 4. Residual link lifetime: analytical and simulation results.

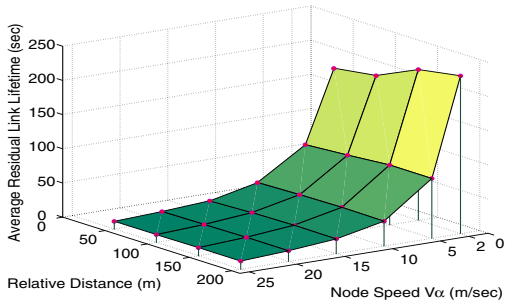

Fig. 5. Average residual link lifetime $\overline{T}_R$, where $R_e = 250$ m.

Based on (14), Fig. 4(a) illustrates both theoretical and simulation PMF of T_R with respect to initial node-pair distance, where v_α= 10 m/s and R_e=250 m. We notice that there always exists a peak for the PMF distribution of the residual link lifetime. Moreover, the peak of the PMF curve shifts towards right side as the initial node-pair distance decreases. Given the initial 200 m node-pair distance, Fig. 4(b) illustrates the expected residual link lifetime $\overline{T}_R$ versus node mobility under different ETRs by simulations. It turns out $\overline{T}_R$ is much more sensitive to the node mobility than the transmission range. Again, by comparing Fig. 3(d) with Fig. 3(d), it is clear that ETR has similar impact on both $\overline{T}_L$ and $\overline{T}_R$.

Furthermore, we investigate the impact of relative distance on average residual link lifetime $\overline{T}_R$ with respect to different node mobility level, where R_e=250 m. The initial node-pair distance is respectively chosen from $\{50, 100, 150, 200\}$ m, when the link is connected. The results of $\overline{T}_R$ obtained through the statistical analysis of simulation data are illustrated in Fig. 5. It is interesting to find that given a specific speed, the $\overline{T}_R$ is almost same regardless the initial node-pair distance, especially when the node speed is high. Therefore, by combining the observation from Fig. 4(b) and Fig. 5, we conclude that the impacting factors on residual link lifetime are in the decreasing order of node speed, transmission range, node-pair distance.

V. Conclusion

In this paper, we presented an in-depth analysis of link statistics regarding link stability and availability in mobile ad hoc networks upon the interactions among radio channel fadings, transmission range, node mobility, and the node-pair distance. The derived stochastic link properties can be readily used for adaptive routing optimization, e.g., how to select a stable path based on link availability prediction and how to properly update routing cache based on the link stability $\overline{T}_{link}$. Our analytical approach also provides a fundamental methodology for investigating MANET issues such as topology control and performance evaluation under both radio channel models and mobility models.

References

[1] M. Zhao and W. Wang, "A novel semi-markov smooth mobility model for mobile ad hoc networks," in *Proc. of IEEE GLOBECOM*, 2006.

[2] M. Gerharz, C. Waal, M.Frank, and P. Martini, "Link stability in mobile wireless ad hoc networks," in *Proc. of IEEE Local Computer Networks LCN*, 2002.

[3] N. Sadagopan, F. Bai, B. Krishnamachari, and A. Helmy, "Paths: Analysis of path duration statistics and their impact on reactive manet routing protocols," in *Proc. of ACM MobiHoc*, June 2003.

[4] P. Samar and S. B. Wicker, "On the behavior of communication links of node in a multi-hop mobile environment," in *Proc. of ACM MobiHoc*, May 2004.

[5] S. Xu, K. Blackmore, and H. Jones, "Assessment for manets requiring persistent links," in *Proc. of International Workshop on WitMeMo*, 2005.

[6] A. B. McDonald and T. F. Znati, "A mobility-based framework for adaptive clustering in wireless ad hoc networks," *IEEE Journal on Selected Areas in Communications*, vol. 17, no. 8, pp. 1466–1487, August 1999.

[7] S. Jiang, "An enhanced prediction-based link availability estimation for manets," *IEEE Transactions on Communications*, vol. 52, no. 2, pp. 183–186, Febuary 2004.

[8] T. Camp, J. Boleng, and V. Davies, "A survey of mobility models for ad hoc networks research," *Wireless Communication and Mobile Computing (WCMC): Special issue on Mobile Ad Hoc Networking: Research, Trends and Applications*, vol. 2, no. 5, pp. 483–502, 2002.

[9] M. Schwartz, *Mobile Wireless Commnications*, 1st ed. CAMBRIDGE, 2005.

[10] C. E. Koksal, K. Jamieson, E. Telatar, and P. Thiran, "Impacts of Channel Variability on Link-Level Throughput in Wireless Networks," in *Proc. of SIGMetrics Perfromance*, 2006.

[11] C. Bettstetter and C. Hartmann, "Connectivity of wireless multihop networks in a shadow fading environment," *ACM/Kluwer Wireless Networks*, vol. 11, no. 5, pp. 571–579, September 2005.

[12] L. Booth, J. Bruck, M. Cook, and M. Franceschetti, "Ad hoc wireless networks with noisy links," in *Proc. of ISIT*, 2003.

[13] M. Zhao and W. Wang, "Analyzing topology dynamics in ad hoc networks using a smooth mobility model," in *Proc. of IEEE WCNC*, 2007.